Supplemental Fig. 1

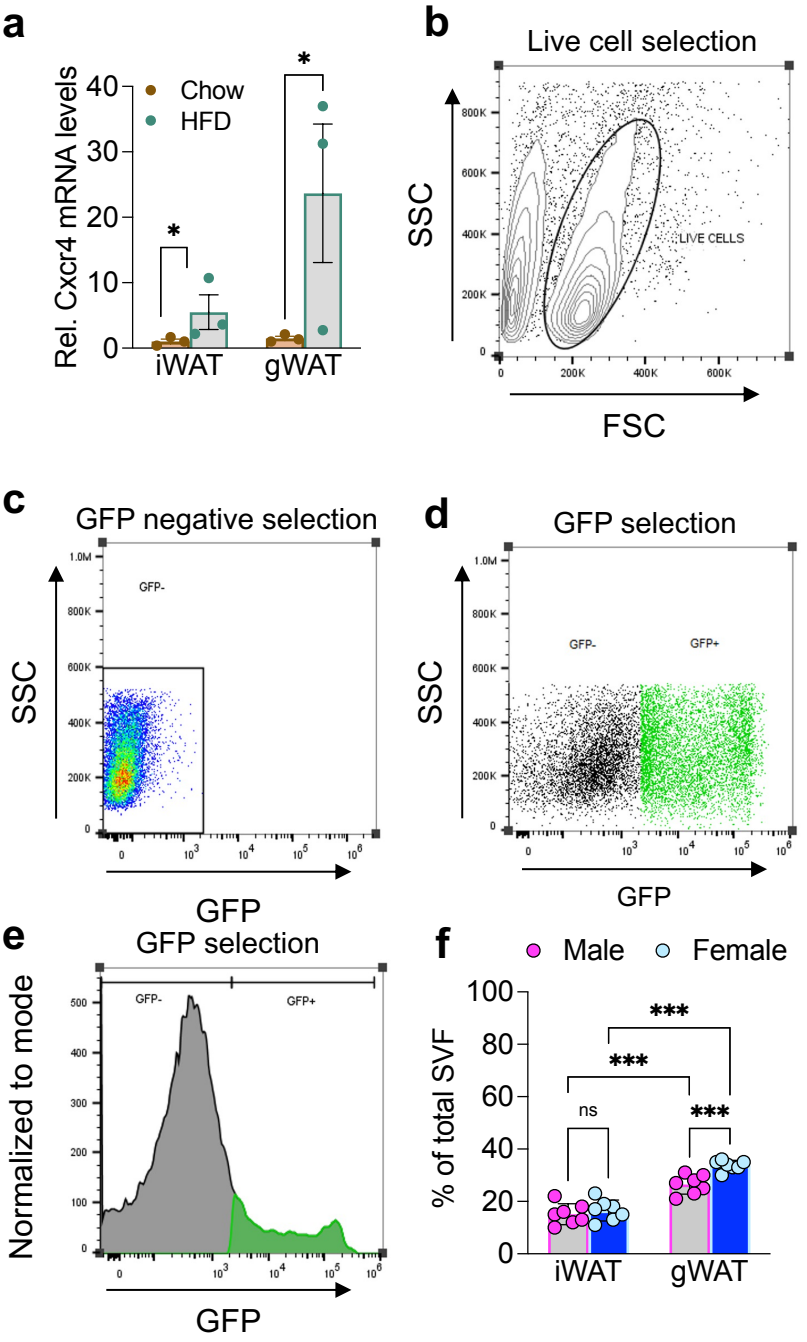

Supplemental Fig. 1: a C57BL/6J mice were fed a normal chow diet or high-fat diet (HFD) for 12 weeks and Cxcr4 mRNA expression was measured within iWAT and gWAT depots. **b** Representative flow plots of live cell selection for analysis. **c** Representative flow plot of an AT-GFP negative mouse model for gating strategy. **d,e** Representative flow plot (**d**) and histogram (**e**) for AT-GFP+ cell selection, gating, and collecting. **f** Total AT-GFP labeled APC populations within iWAT and gWAT depots from male and female mice (n=7 mice/group).

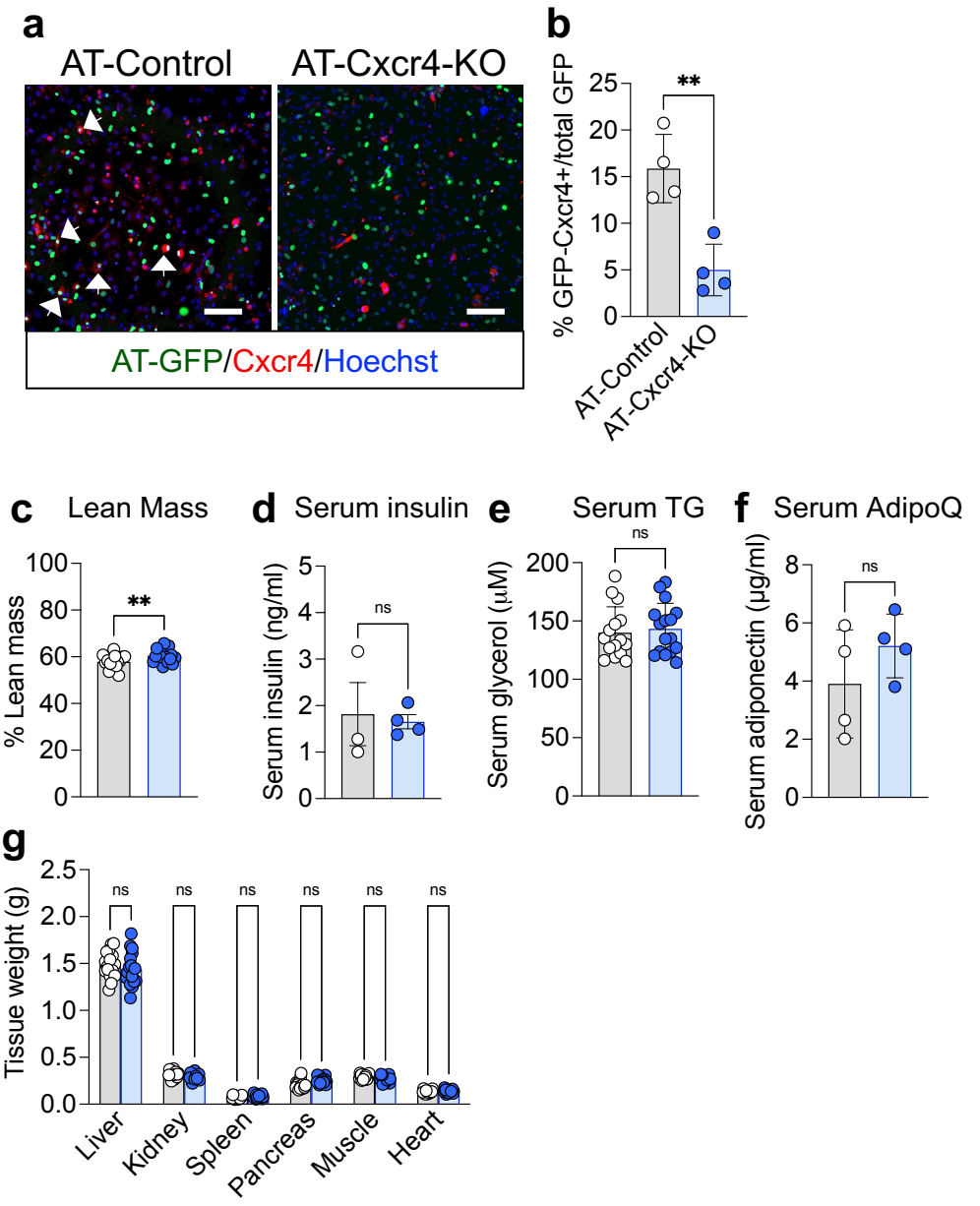

Supplemental Fig. 2: a Representative images of Cxcr4 immunostaining within AT-Control and AT-Cxcr4-KO SVF cultures. Note Cxcr4 positive signal within in GFP AT-Controls but not within AT-Cxcr4-KO APCs. White arrows indicate Cxcr4+ APCs. **b** Image quantification of cultures described in (**a**), examining Cxcr4 presence within GFP+ APCs. **P=0.002 control compared to mutant. Scale bar = 100 µm. **c-g** Two-month-old AT-Control and AT-Cxcr4-KO male mice (n= 16-18/group) were phenotypically evaluated for lean mass (**c**), serum insulin (n= 3-4/group) (**d**), serum triglycerides (TG) (**e**), serum adiponectin (**f**), and organ weight (**g**). Data are means ±S.E.M; **P=0.002; ns= not significant by two-way ANOVA controls compared to mutants.

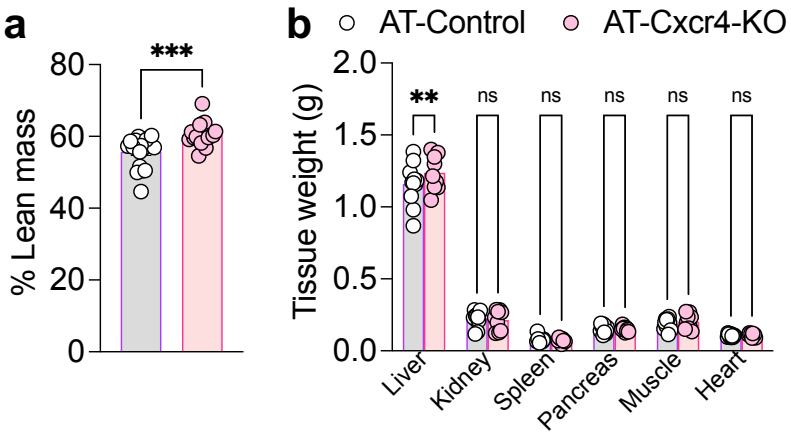

Supplemental Fig. 3: a Two-month-old AT-Control and AT-Cxcr4-KO female mice were phenotypically evaluated for lean mass (n= 14-18/group) (**a**) and organ weight (n= 9-11/group) (**b**). Data are means ±S.E.M; **P=0.002 ***P=0.001; ns= not significant by two-way ANOVA.

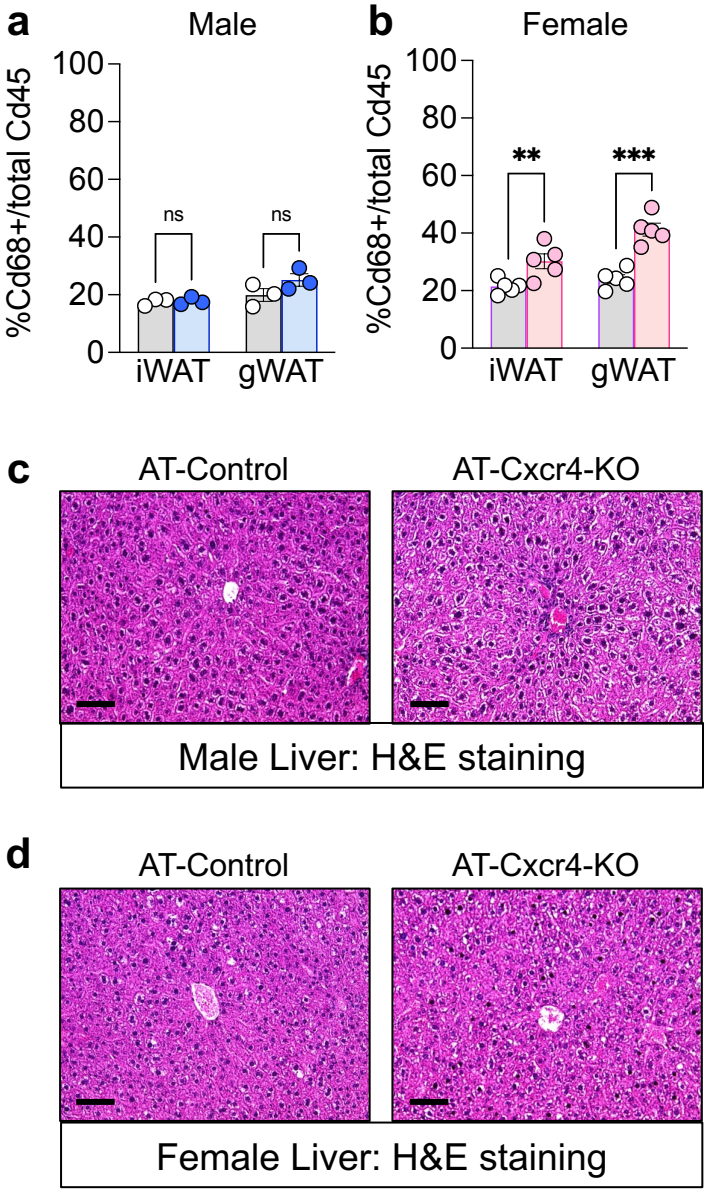

Supplemental Fig. 4: a,b iWAT and gWAT depots from two-month-old AT-Control and AT-Cxcr4-KO male (**a**) and female (**b**) mice were FACS evaluated for Cd68+ macrophage numbers (n= 3-4 mice/group). **c,d** Representative images of H&E staining of liver sections from male and female mice described in (**a**). Data are means ±S.E.M; **P=0.002; ***P=0.001; n= 3 mice/group, ns= not significant by two-way ANOVA mutant compared to control. Scale bar = 100 μm.

Supplemental Fig. 5

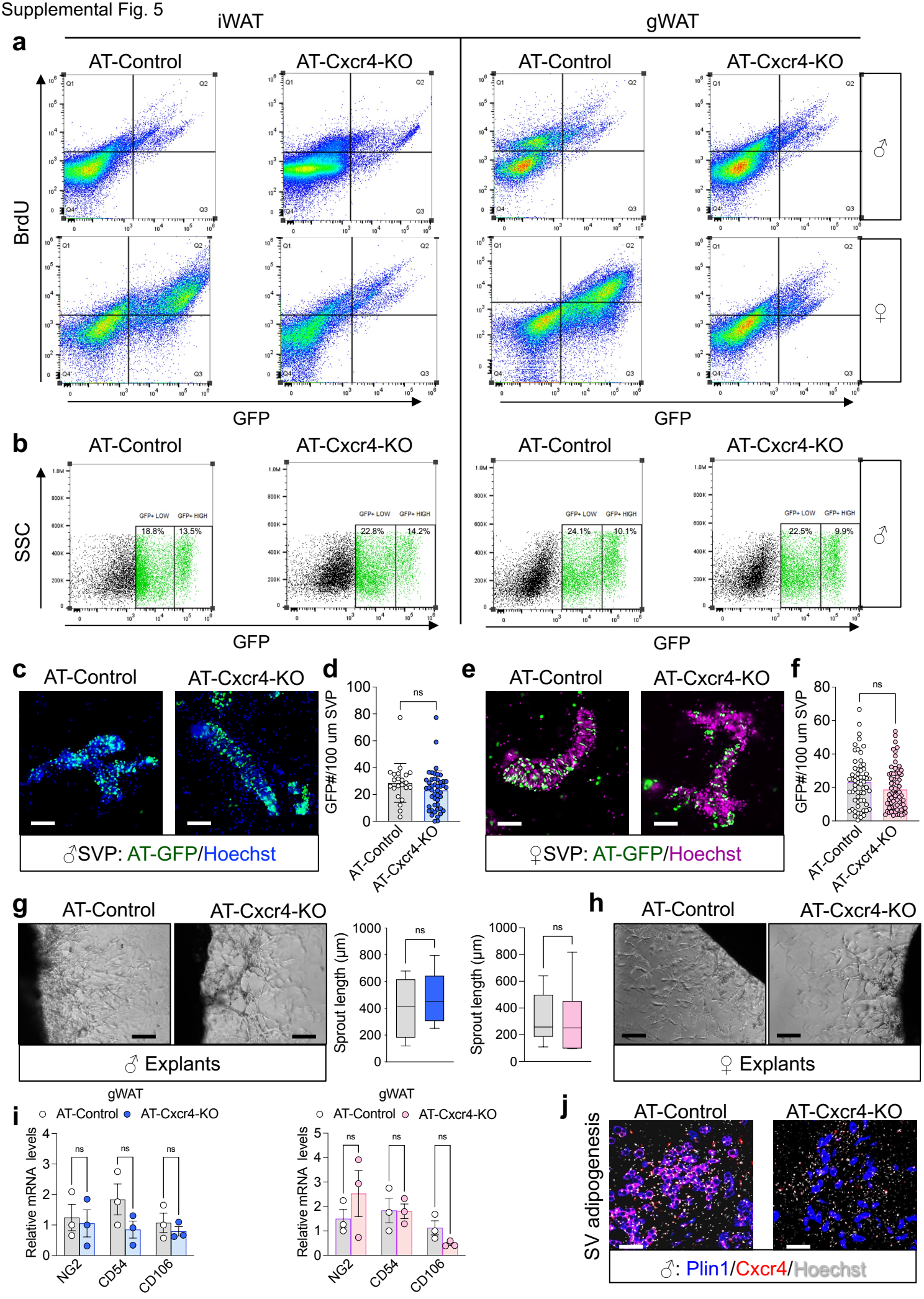

Supplemental Fig. 5: a Representative flow plots of BrdU incorporation (pulse: 5-day administration) within AT-GFP APCs from male (top) and female (bottom) from two-month-old AT-Control and AT-Cxcr4-KO iWAT and gWAT depots. **b** Representative flow profiles of male AT-Control and AT-Cxcr4-KO GFP-labeled APCs within iWAT and gWAT depots. **c-f** Representative images of iWAT SVPs isolated from AT-Control and AT-Cxcr4-KO male (**c**) and female (**e**) mice. Number of GFP+ APCs were quantified per 100 μm of SVP for both male (**d**) and female (**f**) mice (n= 3 mice/group 8-10 SVPs/mouse). **g,h** Representative images of iWAT explants from male (**g**) and female (**h**) AT-Control and AT-Cxcr4-KO mice. Explants were encased in Matrigel and vascular sprout length was assessed and quantified (n= 3 mice/group) 5 days later (**h**). **i** mRNA expression of denoted vascular genes in gWAT depots from male and female AT-Control and AT-Cxcr4-KO mice. **j** Representative immunostaining images of perilipin (Plin1) and Cxcr4 from male AT-Control and AT-Cxcr4-KO adipogenic cultures. Data are means ±S.E.M;, ns= not significant by two-way ANOVA. Scale bar = 100 μm.

Supplemental Fig. 6

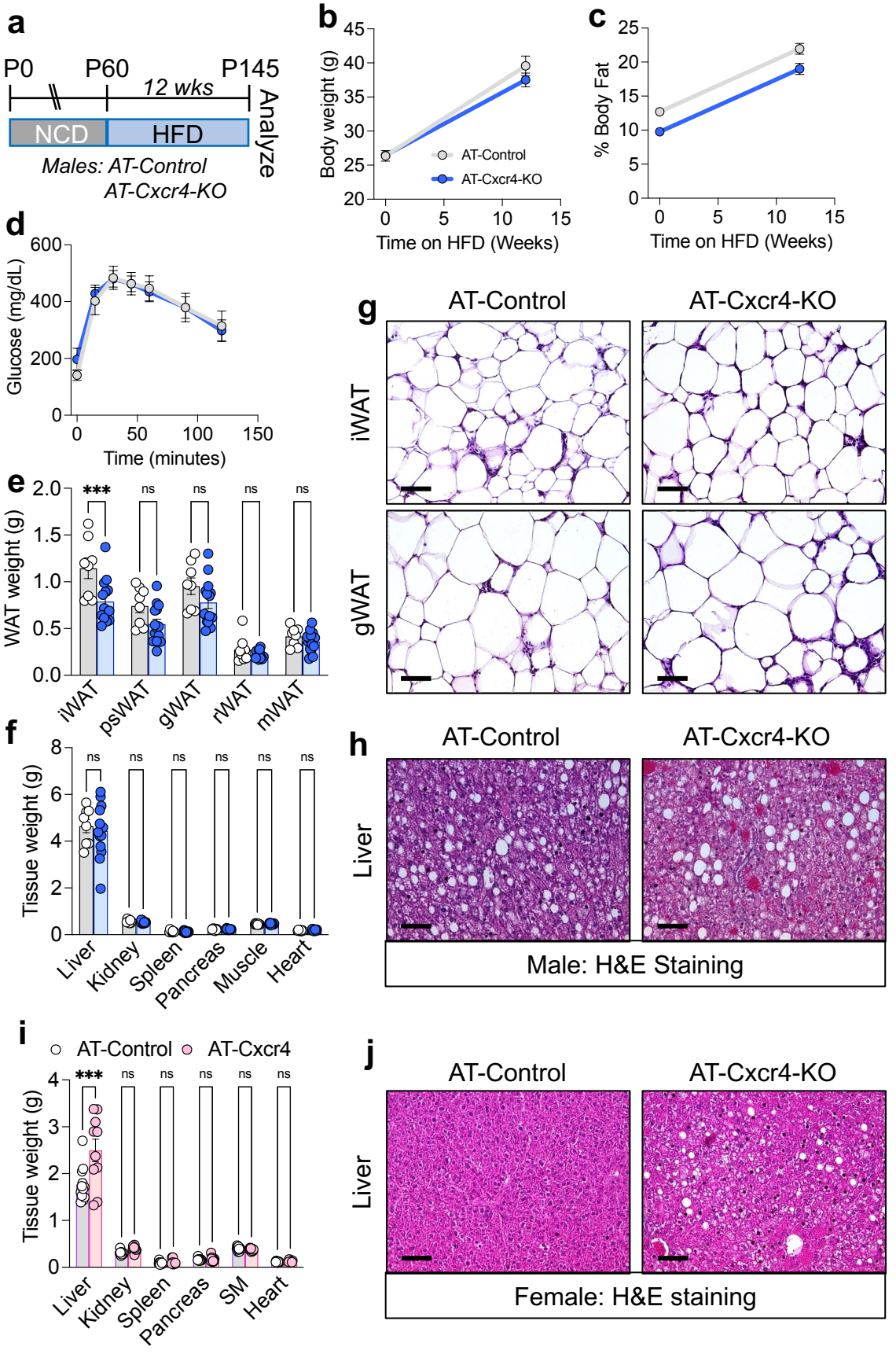

Supplemental Fig. 6: a-d Experimental schema: Two-month-old male AT-Control and AT-Cxcr4-KO male mice were fed a HFD for 12 weeks (**a**) (n= 8, 14 mice/group) and were phenotypically assessed for body weight gain (**b**), adiposity (**c**), glucose tolerance (**d**), WAT weight (**e**), and organ weight (**f**). **g,h** Representative images of H&E staining of iWAT, gWAT, and liver from mice described in (**a**). **i,j** AT-Control and AT-Cxcr4-KO female mice were fed a HFD for 12 weeks. Tissue weights (**i**) and liver histology (**j**) were evaluated. Data are means ±S.E.M; ***P=0.001; ns= not significant by two-way ANOVA control compared to mutant. Scale bar = 100 μm.

Supplemental Fig. 7

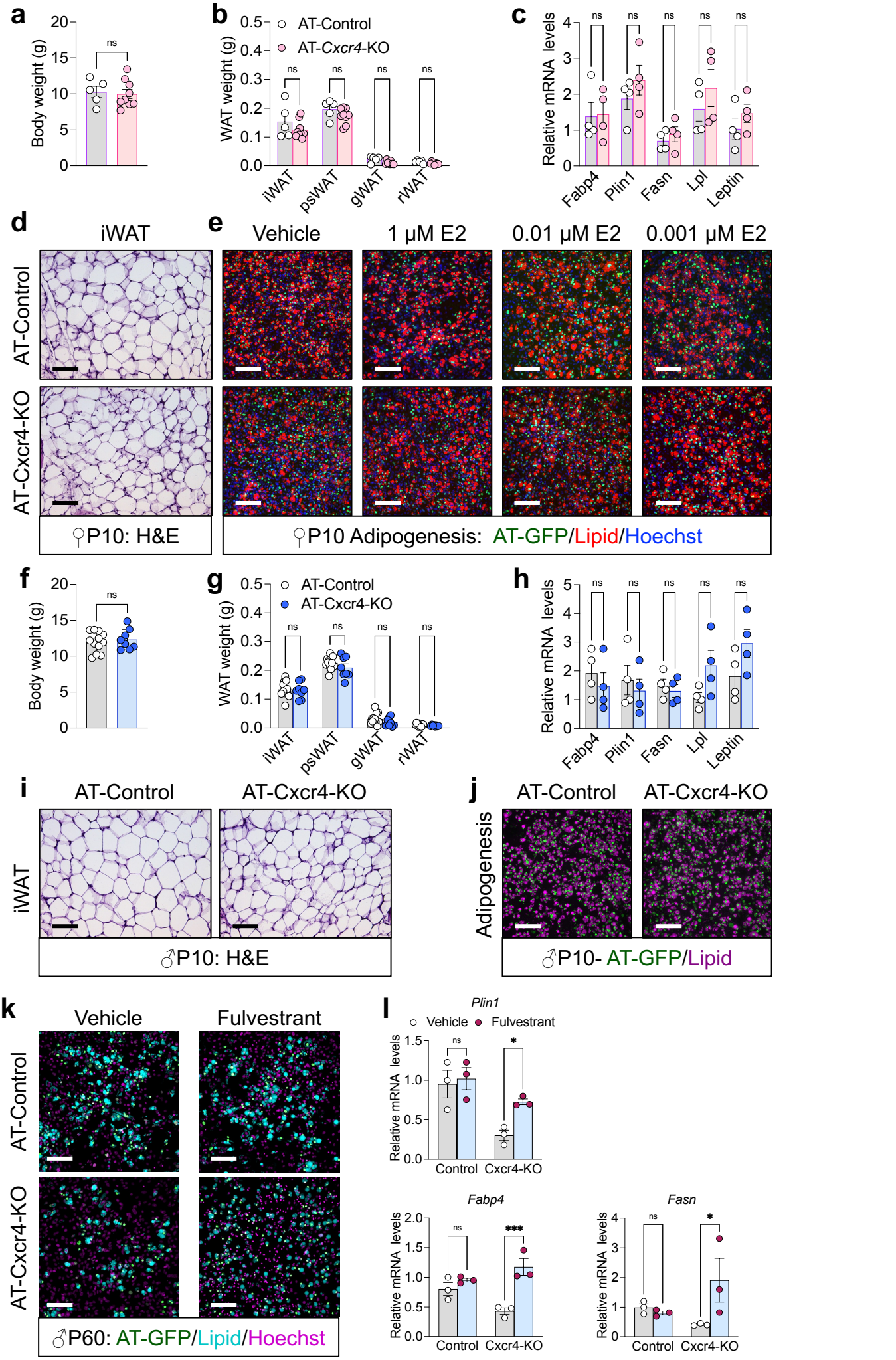

Supplemental Fig. 7: a-d AT-Control and AT-Cxcr4-KO female mice (n= 5, 9/group) were phenotypically evaluated at postnatal day 10 for: body weight (**a**), WAT weight (**b**), adipocyte gene expression (**c**) (n= 4/group), and iWAT histology (H&E staining) (**d**). **e** Representative images of in vitro adipogenesis from iWAT SV cells from mice described in (**a**). Cells were treated with adipogenic media with denoted concentrations of 17β-estradiol (E2) throughout differentiation. Differentiation was assessed by lipidTox staining. **f-i** AT-Control and AT-Cxcr4-KO male mice were phenotypically evaluated at postnatal day 10 for: body weight (**f**), WAT weight (**g**), adipocyte gene expression (**h**), and iWAT histology (H&E staining) (**i**). **j** Representative images of in vitro adipogenesis from iWAT SV cells from mice described in (**f**). Differentiation was assessed by lipidTox staining. **k,l** SV cells were isolated from iWAT depots from two-month-old male AT-Control and AT-Cxcr4-KO mice (n= 3/group). Cells were induced with adipogenic media along with vehicle or fulvestrant (1 μm). Adipogenesis was assessed by lipidTox staining (**k**) and mRNA expression (**l**). Data are means ±S.E.M; *P=0.033, ***P=0.001 , and ns= not significant by two-way ANOVA vehicle treated mutant cells compared to fulvestrant treated mutant cells. Scale bar = 100 μm.

Supplemental Fig. 8

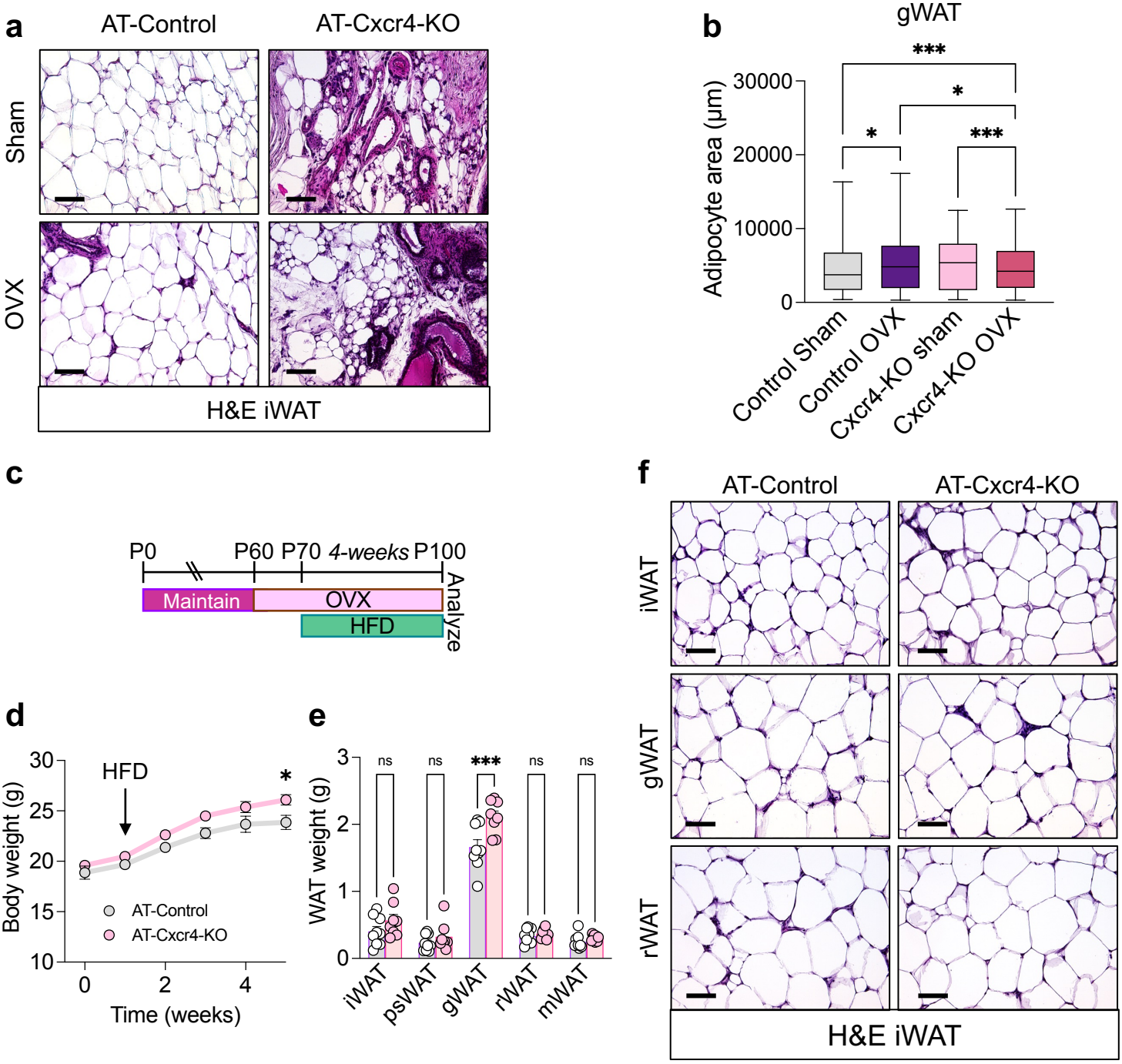

Supplemental Fig. 8: a Representative H&E images of iWAT depot sections from sham or OVX AT-Control and AT-Cxcr4-KO female mice. **b** Image quantification of adipocyte area from gWAT sections from sham and ovariectomized AT-Control and AT-Cxcr4-KO female mice. **c-f** Experimental schema (**c**): Two-month-old AT-Control and AT-Cxcr4-KO mice were ovariectomized (n= 9, 8/group). One-week post-surgery mice were fed a HFD for 4 weeks and subsequently evaluated for: body weight (**d**), WAT weight (**e**), and WAT histology (H&E staining) (**f**). Data are means ±S.E.M; *P=0.033; **P=0.002; ***P=0.001 by two-way ANOVA controls compared to mutants. Scale bar = 100 μm.

Supplemental Table 1: qPCR primer list

Gene	Forward	Reverse
AdipoQ	TGTTCCTCTTAATCCTGCCCA	CCAACCTGCACAAGTTCCCTT
Ccl2	TTAAAAACCTGGATCGGAACCAA	GCATTAGCTTCAGATTTACGGGT
Cd54	CACAGTTCTCAAAGCACAGCG	GTGATGCTCAGGTATCCATCC
Cd106	AGTTGGGGATTCGGTTGTTCT	CCCCTCATTCCTTACCACCC
Col1α1	GGAGAGTACTGGATCGACCCTAAC	ACACAGGTCTGACCTGTCTCCAT
Col3a1	GTGCTCCTGGACAGAATGGT	CACCCTTTACACCCTGAGGA
Col4a1	GCCAAGTGTGCATGAGAAGA	AGCGGGGTGTGTTAGTTACG
Cxcr4	CTTCTGGGCAGTTGATGCCCAT	CTGTTGGTGGCGTGGACAAT
Esr1	CCTCCCGCCTTCTACAGGT	CACACGGCACAGTAGCGAG
Esr2	CTGTGATGAACTACAGTGTTCCC	CACATTTGGGCTTGCAGTCTG
F4/80	TGACTCACCTTGTGGTCCTAA	CTTCCCAGAATCCAGTCTTTCC
Fabp4	AAGGTGAAGAGCATCATAACCCT	TCACGCCTTTCATAACACATTCC
Fasn	GGAGGTGGTGATAGCCGGTAT	TGGGTAATCCATAGAGCCCAG
Fbln2	CTGTGAAGACCAAGACGAGTG	CGTTGAGGATATAGCCCTCTGC
Gper	ATGGATGCGACTACTCCAGC	AAGAGGGCAATCACGTACTGC
Il-6	GGTGACAACCACGGCCTTCCC	AAGCCTCCGACTTGTGAAGTGGT
Leptin	GAGACCCCTGTGTCGGTTC	CTGCGTGTGTGAAATGTCATTG
Lpl	CATCGAGAGAGGATCCGAGTGAA	TGCTGAGTCCTTTCCCTTCTG
Ng2 (CSPG4)	GGGCTGTGCTGTCTGTTGA	TGATTCCCTTCAGGTAAGGCA
Tnfa	CCCTCACACTCAGATCATCTTCT	GCTACGACGTGGGCTACAG
Perilipin	GGGACCTGTGAGTGCTTCC	GTATTGAAGAGCCGGGATCTTTT
Pparγ	TCGCTGATGCACTGCCTATG	GAGAGGTCCACAGAGCTGATT
Rn18S	GTAACCCGTTGAACCCCATT	CCATCCAATCGGTAGTAGCG